

Narrowing of the Balance Function with Centrality in Au + Au Collisions at $\sqrt{s_{NN}} = 130$ GeV

J. Adams,³ C. Adler,¹¹ Z. Ahammed,²³ C. Allgower,¹² J. Amonett,¹⁴ B. D. Anderson,¹⁴ M. Anderson,⁵ G. S. Averichev,⁹ J. Balewski,¹² O. Barannikova,^{9,23} L. S. Barnby,¹⁴ J. Baudot,¹³ S. Bekele,²⁰ V. V. Belaga,⁹ R. Bellwied,³¹ J. Berger,¹¹ H. Bichsel,³⁰ A. Billmeier,³¹ L. C. Bland,² C. O. Blyth,³ B. E. Bonner,²⁴ A. Boucham,²⁶ A. Brandin,¹⁸ A. Bravar,² R. V. Cadman,¹ H. Caines,³³ M. Calderón de la Barca Sánchez,² A. Cardenas,²³ J. Carroll,¹⁵ J. Castillo,¹⁵ M. Castro,³¹ D. Cebra,⁵ P. Chaloupka,²⁰ S. Chattopadhyay,³¹ Y. Chen,⁶ S. P. Chernenko,⁹ M. Cherney,⁸ A. Chikanian,³³ B. Choi,²⁸ W. Christie,² J. P. Coffin,¹³ T. M. Cormier,³¹ M. M. Corral,¹⁶ J. G. Cramer,³⁰ H. J. Crawford,⁴ A. A. Derevschikov,²² L. Didenko,² T. Dietel,¹¹ J. E. Draper,⁵ V. B. Dunin,⁹ J. C. Dunlop,³³ V. Eckardt,¹⁶ L. G. Efimov,⁹ V. Emelianov,¹⁸ J. Engelage,⁴ G. Eppley,²⁴ B. Erazmus,²⁶ P. Fachini,² V. Faine,² J. Faivre,¹³ R. Fatemi,¹² K. Filimonov,¹⁵ E. Finch,³³ Y. Fisyak,² D. Flierl,¹¹ K. J. Foley,² J. Fu,^{15,32} C. A. Gagliardi,²⁷ N. Gagunashvili,⁹ J. Gans,³³ L. Gaudichet,²⁶ M. Germain,¹³ F. Geurts,²⁴ V. Ghazikhanian,⁶ O. Grachov,³¹ V. Grigoriev,¹⁸ M. Guedon,¹³ S. M. Guertin,⁶ E. Gushin,¹⁸ T. J. Hallman,² D. Hardtke,¹⁵ J. W. Harris,³³ M. Heinz,³³ T. W. Henry,²⁷ S. Heppelmann,²¹ T. Herston,²³ B. Hippolyte,¹³ A. Hirsch,²³ E. Hjort,¹⁵ G. W. Hoffmann,²⁸ M. Horsley,³³ H. Z. Huang,⁶ T. J. Humanic,²⁰ G. Igo,⁶ A. Ishihara,²⁸ Yu. I. Ivanshin,¹⁰ P. Jacobs,¹⁵ W. W. Jacobs,¹² M. Janik,²⁹ I. Johnson,¹⁵ P. G. Jones,³ E. G. Judd,⁴ M. Kaneta,¹⁵ M. Kaplan,⁷ D. Keane,¹⁴ J. Kiryluk,⁶ A. Kisiel,²⁹ J. Klay,¹⁵ S. R. Klein,¹⁵ A. Klyachko,¹² T. Kollegger,¹¹ A. S. Konstantinov,²² M. Kopytine,¹⁴ L. Kotchenda,¹⁸ A. D. Kovalenko,⁹ M. Kramer,¹⁹ P. Kravtsov,¹⁸ K. Krueger,¹ C. Kuhn,¹³ A. I. Kulikov,⁹ G. J. Kunde,³³ C. L. Kunz,⁷ R. Kh. Kutuev,¹⁰ A. A. Kuznetsov,⁹ M. A. C. Lamont,³ J. M. Landgraf,² S. Lange,¹¹ C. P. Lansdell,²⁸ B. Lasiuk,³³ F. Laue,² J. Lauret,² A. Lebedev,² R. Lednický,⁹ V. M. Leontiev,²² M. J. LeVine,² Q. Li,³¹ S. J. Lindenbaum,¹⁹ M. A. Lisa,²⁰ F. Liu,³² L. Liu,³² Z. Liu,³² Q. J. Liu,³⁰ T. Ljubicic,² W. J. Llope,²⁴ H. Long,⁶ R. S. Longacre,² M. Lopez-Noriega,²⁰ W. A. Love,² T. Ludlam,² D. Lynn,² J. Ma,⁶ D. Magestro,²⁰ R. Majka,³³ S. Margetis,¹⁴ C. Markert,³³ L. Martin,²⁶ J. Marx,¹⁵ H. S. Matis,¹⁵ Yu. A. Matulenko,²² T. S. McShane,⁸ F. Meissner,¹⁵ Yu. Melnick,²² A. Meschanin,²² M. Messer,² M. L. Miller,³³ Z. Milosevich,⁷ N. G. Minaev,²² J. Mitchell,²⁴ C. F. Moore,²⁸ V. Morozov,¹⁵ M. M. de Moura,³¹ M. G. Munhoz,²⁵ J. M. Nelson,³ P. Nevski,² V. A. Nikitin,¹⁰ L. V. Nogach,²² B. Norman,¹⁴ S. B. Nurushev,²² G. Odyniec,¹⁵ A. Ogawa,² V. Okorokov,¹⁸ M. Oldenburg,¹⁶ D. Olson,¹⁵ G. Paic,²⁰ S. U. Pandey,³¹ Y. Panebratsev,⁹ S. Y. Panitkin,² A. I. Pavlinov,³¹ T. Pawlak,²⁹ V. Perevoztchikov,² W. Peryt,²⁹ V. A. Petrov,¹⁰ M. Planinic,¹² J. Pluta,²⁹ N. Porile,²³ J. Porter,² A. M. Poskanzer,¹⁵ E. Potrebenikova,⁹ D. Prindle,³⁰ C. Pruneau,³¹ J. Putschke,¹⁶ G. Rai,¹⁵ G. Rakness,¹² O. Ravel,²⁶ R. L. Ray,²⁸ S. V. Razin,^{9,12} D. Reichhold,²³ J. G. Reid,³⁰ G. Renault,²⁶ F. Retiere,¹⁵ A. Ridiger,¹⁸ H. G. Ritter,¹⁵ J. B. Roberts,²⁴ O. V. Rogachevski,⁹ J. L. Romero,⁵ A. Rose,³¹ C. Roy,²⁶ V. Rykov,³¹ I. Sakrejda,¹⁵ S. Salur,³³ J. Sandweiss,³³ I. Savin,¹⁰ J. Schambach,²⁸ R. P. Scharenberg,²³ N. Schmitz,¹⁶ L. S. Schroeder,¹⁵ A. Schüttauf,¹⁶ K. Schweda,¹⁵ J. Seger,⁸ D. Seliverstov,¹⁸ P. Seyboth,¹⁶ E. Shahaliev,⁹ K. E. Shestermanov,²² S. S. Shimanskii,⁹ F. Simon,¹⁶ G. Skoro,⁹ N. Smirnov,³³ R. Snellings,¹⁵ P. Sorensen,⁶ J. Sowinski,¹² H. M. Spinka,¹ B. Srivastava,²³ E. J. Stephenson,¹² R. Stock,¹¹ A. Stolpovsky,³¹ M. Strikhanov,¹⁸ B. Stringfellow,²³ C. Struck,¹¹ A. A. P. Suaide,³¹ E. Sugarbaker,²⁰ C. Suire,² M. Šumbera,²⁰ B. Surov,² T. J. M. Symons,¹⁵ A. Szanto de Toledo,²⁵ P. Szarwas,²⁹ A. Tai,⁶ J. Takahashi,²⁵ A. H. Tang,¹⁵ D. Thein,⁶ J. H. Thomas,¹⁵ M. Thompson,³ V. Tikhomirov,¹⁸ M. Tokarev,⁹ M. B. Tonjes,¹⁷ T. A. Trainor,³⁰ S. Trentalange,⁶ R. E. Tribble,²⁷ V. Trofimov,¹⁸ O. Tsai,⁶ T. Ullrich,² D. G. Underwood,¹ G. Van Buren,² A. M. Vander Molen,¹⁷ I. M. Vasilevski,¹⁰ A. N. Vasiliev,²² S. E. Vigdor,¹² S. A. Voloshin,³¹ F. Wang,²³ H. Ward,²⁸ J. W. Watson,¹⁴ R. Wells,²⁰ G. D. Westfall,¹⁷ C. Whitten, Jr.,⁶ H. Wieman,¹⁵ R. Willson,²⁰ S. W. Wissink,¹² R. Witt,³³ J. Wood,⁶ N. Xu,¹⁵ Z. Xu,² A. E. Yakutin,²² E. Yamamoto,¹⁵ J. Yang,⁶ P. Yepes,²⁴ V. I. Yurevich,⁹ Y. V. Zanevski,⁹ I. Zborovský,⁹ H. Zhang,³³ W. M. Zhang,¹⁴ R. Zoukarneev,¹⁰ and A. N. Zubarev⁹

(STAR Collaboration)

¹Argonne National Laboratory, Argonne, Illinois 60439, USA²Brookhaven National Laboratory, Upton, New York 11973, USA³University of Birmingham, Birmingham, United Kingdom⁴University of California, Berkeley, California 94720, USA⁵University of California, Davis, California 95616, USA⁶University of California, Los Angeles, California 90095, USA⁷Carnegie Mellon University, Pittsburgh, Pennsylvania 15213, USA⁸Creighton University, Omaha, Nebraska 68178, USA⁹Laboratory for High Energy (JINR), Dubna, Russia

- ¹⁰Particle Physics Laboratory (JINR), Dubna, Russia
¹¹University of Frankfurt, Frankfurt, Germany
¹²Indiana University, Bloomington, Indiana 47408, USA
¹³Institut de Recherches Subatomiques, Strasbourg, France
¹⁴Kent State University, Kent, Ohio 44242, USA
¹⁵Lawrence Berkeley National Laboratory, Berkeley, California 94720, USA
¹⁶Max-Planck-Institut fuer Physik, Munich, Germany
¹⁷Michigan State University, East Lansing, Michigan 48824, USA
¹⁸Moscow Engineering Physics Institute, Moscow Russia
¹⁹City College of New York, New York City, New York 10031, USA
²⁰Ohio State University, Columbus, Ohio 43210, USA
²¹Pennsylvania State University, University Park, Pennsylvania 16802, USA
²²Institute of High Energy Physics, Protvino, Russia
²³Purdue University, West Lafayette, Indiana 47907, USA
²⁴Rice University, Houston, Texas 77251, USA
²⁵Universidade de Sao Paulo, Sao Paulo, Brazil
²⁶SUBATECH, Nantes, France
²⁷Texas A&M University, College Station, Texas 77843, USA
²⁸University of Texas, Austin, Texas 78712, USA
²⁹Warsaw University of Technology, Warsaw, Poland
³⁰University of Washington, Seattle, Washington 98195, USA
³¹Wayne State University, Detroit, Michigan 48201, USA
³²Institute of Particle Physics, CCNU (HZNU), Wuhan, 430079 China
³³Yale University, New Haven, Connecticut 06520, USA
(Received 23 January 2003; published 2 May 2003)

The balance function is a new observable based on the principle that charge is locally conserved when particles are pair produced. Balance functions have been measured for charged particle pairs and identified charged pion pairs in Au + Au collisions at $\sqrt{s_{NN}} = 130$ GeV at the Relativistic Heavy Ion Collider using STAR. Balance functions for peripheral collisions have widths consistent with model predictions based on a superposition of nucleon-nucleon scattering. Widths in central collisions are smaller, consistent with trends predicted by models incorporating late hadronization.

DOI: 10.1103/PhysRevLett.90.172301

PACS numbers: 25.75.Gz

Collisions of Au nuclei at ultrarelativistic energies can produce large energy densities and high temperatures. At these densities and temperatures, the produced matter may be best portrayed by partonic (quark/gluon) degrees of freedom as opposed to those characterizing a hot hadronic phase. This partonic phase would necessarily be followed by a transition to normal hadronic particles, which are ultimately measured [1]. Numerous probes of the high density medium have been proposed [2], including observables related to fluctuations and correlations [3–7].

One such observable, the balance function, is sensitive to whether the transition to a hadronic phase was delayed, as expected if the quark-gluon phase were to persist for a substantial time [8]. The authors of Ref. [8] formulate the balance function as follows in this paragraph. As a result of local charge conservation, when particles and their antiparticles are pair produced, they are correlated initially in coordinate space. If hadronization occurs early, the members of a charge/anticharge pair would be expected to separate in rapidity due to expansion and rescattering in the strongly interacting medium. Alternatively, delayed hadronization would lead to a stronger correlation in rapidity between the particles of

charge/anticharge pairs in the final state. Measuring this correlation involves subtracting uncorrelated charge/anticharge pairs on an event-by-event basis. The remaining charge/anticharge particle pairs are examined to determine the correlation as a function of the relative rapidity, Δy , between the members of the pairs. The balance function is expected to be narrower for a scenario with delayed hadronization, and is therefore sensitive to the conjecture that a quark-gluon plasma may be produced.

The balance function is a new observable for heavy ion collisions. This function is similar in form to what is used in [9] to study the charged balance from both $p + p$ and $e^+ + e^-$ collisions [10].

In this analysis, the balance function is used to examine the pseudorapidity correlation of nonidentified charged particles and the rapidity correlation of identified charged pions. The balance function is calculated as

$$B = \frac{1}{2} \left\{ \frac{\Delta_{+-} - \Delta_{++}}{N_+} + \frac{\Delta_{-+} - \Delta_{--}}{N_-} \right\}, \quad (1)$$

where Δ_{+-} in the case of identified charged pion pairs denotes the number of identified charged pion pairs in a given rapidity range $\Delta y = |y(\pi^+) - y(\pi^-)|$, similarly

for Δ_{++} , Δ_{--} , and Δ_{+-} . In the case of nonidentified charged particle pairs, pseudorapidity (η) is used. The terms Δ_{+-} , Δ_{++} , Δ_{--} , and Δ_{-+} are calculated using pairs from a given event and the resulting distributions are summed over all events. Specifically, the distribution Δ_{+-} is calculated by taking in turn each positive particle in an event and incrementing a histogram in Δy ($\Delta \eta$) with respect to all the negative particles in that event. The distribution Δ_{+-} is then summed over all events. A similar procedure is followed for Δ_{++} , Δ_{--} , and Δ_{-+} . $N_{+(-)}$ is the number of positive (negative) pions or nonidentified charged particles summed over all events. The balance function is calculated for all charged pion or charged particle pairs for a given centrality bin. The balance function, in addition to being proportional to charge correlations, is also proportional to the average acceptance for each Δy ($\Delta \eta$) bin. Because the acceptance falls with increasing Δy ($\Delta \eta$), the measured balance functions presented here are narrower than model calculations assuming no detector acceptance effects.

The data used in this analysis were measured using the Solenoidal Tracker at RHIC (STAR) detector for Au + Au collisions at $\sqrt{s_{NN}} = 130$ GeV. The main detector used for this analysis was the time projection chamber (TPC) [11] located in a solenoidal magnetic field of 0.25 T [12]. The TPC provided tracking information for charged particles having transverse momentum $p_t > 100$ MeV/c and $|\eta| < 1.3$ with complete azimuthal acceptance. Minimum bias triggers were defined by the coincidence of two zero degree calorimeters (ZDCs) [13] located ± 18 m from the center of the interaction region. Central collision triggers were defined using both the ZDCs and the central trigger barrel (CTB), an array of scintillator slats surrounding the outside of the TPC. A coincidence in the ZDCs accompanied by a signal in the CTB above a threshold empirically determined to correspond to approximately the 15% most central events was used to define the central collision trigger. Centrality bins were determined using the charged particle multiplicity distributions. Central collisions correspond to 0%–10%, midcentral 10%–40%, midperipheral 40%–70%, and peripheral 70%–96% of the integrated total. Only events with five or more tracks in the TPC were used in this analysis.

For this analysis 150 777 minimum bias and 111 142 centrally triggered events were used. Only charged particle tracks having more than 15 space points along the trajectory were accepted. In addition, the reconstructed trajectory was required to point within 1 cm of the primary vertex. To suppress double counting due to track splitting, the ratio of reconstructed space points to possible space points along the track was required to be greater than 0.52. Tracks were further required to have a momentum $0.1 < p < 2$ GeV/c. Simulations of TPC performance indicate the tracking efficiency for tracks within this acceptance and momentum range is 85%–90% [14].

Charged pion identification was accomplished by selecting particles within 2 standard deviations of the expected dE/dx for a given momentum, which provided pion identification for momenta less than 0.7 GeV/c. Kaon contamination of the pions is negligible at low momentum and is estimated to be 5% at 0.7 GeV/c. Electrons were removed by requiring the measured dE/dx to be more than 2 standard deviations away from the expected value for an electron of the measured momentum. An estimated 1% of the electron contamination remains in the pion sample after these cuts are made. The lowest $\Delta \eta$ (Δy) bin, which was estimated to contain 90% of the remaining electron contamination, was not used in the calculation of the width of the balance function.

Theoretical simulations of the balance function for Au + Au collisions at $\sqrt{s_{NN}} = 130$ GeV were carried out using version 1.36 of HIJING [15] with the default settings for impact parameters ranging from 0 to 15 fm. A realistic distribution was used for event vertices within the interaction region. HIJING events were processed using GEANT [16] and the TPC track reconstruction software. The same cuts were applied to the HIJING events that were applied to the data. None of the features of the balance functions computed from the filtered simulations show any dependence on centrality [17]. Thus, the STAR results are compared to HIJING integrated over centrality. Figure 1(a) shows the balance function [Eq. (1)] measured for charged particles for the central and peripheral Au + Au collision samples. The errors shown are statistical. The systematic error in the balance function is estimated to be 5% due to systematic variations in tracking efficiency, the measurement of pseudorapidity, and contamination of electrons. The comparable balance function derived for HIJING events simulated in the STAR detector using GEANT is shown in Fig. 1(b).

The area under the balance function is constrained by global charge conservation and STAR's acceptance [18]. Physical effects over and above this constraint can be discerned by comparison to a reference data set that preserves global charge conservation, while removing effects of dynamical particle correlations. A relevant reference is provided in Fig. 1(b) for central and peripheral collision samples independently by calculating the balance function after the pseudorapidities of all charged particles within each measured event have been randomly shuffled. Dynamical correlations in Au + Au are reflected in the deviation of the results in Fig. 1(a) from the shuffled pseudorapidity results in Fig. 1(b). In addition, Fig. 1(a) also shows the balance functions generated from conventional mixed-event samples constructed [17] by choosing random particles from different measured events with similar event vertex positions and centralities. The balance function for mixed events integrates to zero because global charge conservation has been removed. The fact that the balance function is zero for all $\Delta \eta$ for all centralities demonstrates that STAR's

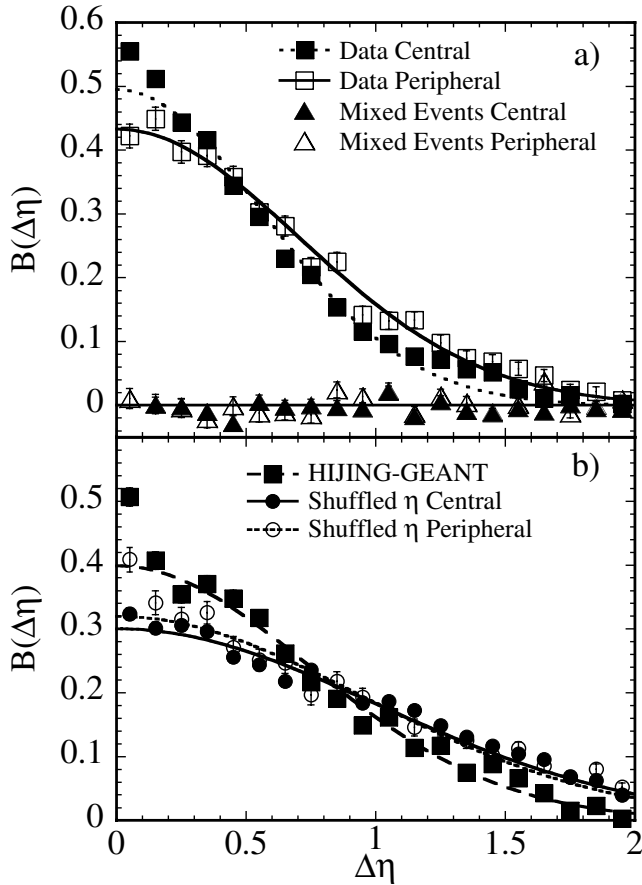


FIG. 1. The balance function versus $\Delta\eta$ for charged particle pairs from (a) central and peripheral Au + Au collisions at $\sqrt{s_{NN}} = 130$ GeV and mixed events from central and peripheral Au + Au collisions, and (b) HIJING events filtered with GEANT [16] and shuffled pseudorapidity events from measured central and peripheral Au + Au collisions. To guide the eye, Gaussian fits excluding the lowest bin in $\Delta\eta$ are shown. The error bars shown are statistical. The balance function for HIJING events is independent of centrality.

acceptance in $\Delta\eta$ is smooth. For both the mixed events and shuffled pseudorapidity samples, the inclusive measured pseudorapidity distributions are preserved.

Within this area constraint, the variation of the balance function with centrality can be effectively characterized by the single parameter $\langle\Delta\eta\rangle$, the mean pseudorapidity difference weighted by the balance function (excluding the lowest bin in $\Delta\eta$ to reduce the background correlation from electron contamination). We refer to $\langle\Delta\eta\rangle$ below as the “width” of the balance function. The measured widths for four centrality classes are shown in Fig. 2 as a function of the impact parameter fraction b/b_{\max} , which is determined using a simple geometrical picture [19] to relate impact parameter to fractions of the total cross section. In Fig. 2, the width of the balance function measured for central collisions is significantly smaller than that for peripheral collisions. The results for the midperipheral and midcentral centrality classes decrease

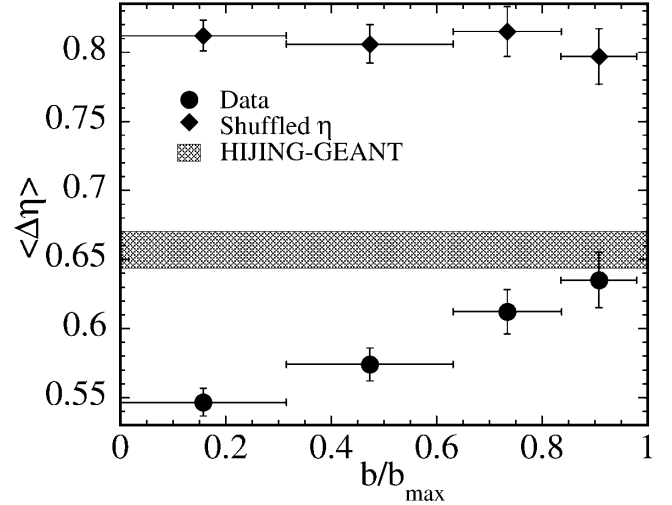


FIG. 2. The width of the balance function for charged particles, $\langle\Delta\eta\rangle$, as a function of normalized impact parameter (b/b_{\max}). Error bars shown are statistical. The width of the balance function from HIJING events is shown as a band whose height reflects the statistical uncertainty. Also shown are the widths from the shuffled pseudorapidity events.

smoothly and monotonically from the peripheral collision value. Figure 2 indicates that, while the width observed in peripheral collisions is consistent with the HIJING prediction, the balance function for central collisions is significantly narrower, suggesting a variation in the underlying particle production dynamics between these two classes of events. In Fig. 2, the widths from the shuffled pseudorapidity events are also shown. These widths show little centrality dependence and are wider than those of the data or HIJING. The widths from shuffled pseudorapidity events represent the maximum possible width of a balance function measured with the STAR detector consistent with no correlations in momentum.

The results for identified charged pion pairs are similar to those for nonidentified charged particles as indicated in Fig. 3. The overall shape of the balance function is similar to that in Fig. 1. However, the data for pions have a dip near $\Delta\eta = 0$ [Fig. 3(a)]. As shown in Ref. [18], this dip can be understood as the combined effect of Bose-Einstein correlations and Coulomb interactions between charged pions. HIJING does not account for these effects, and the balance function predicted in Fig. 3(b) therefore does not show a dip, although the enhancement of the lowest bin due to electron contamination is still apparent.

The width of the balance functions for the four centrality classes is shown in Fig. 4, where the lowest two bins in $\Delta\eta$ have been excluded to avoid the effects of Bose-Einstein correlations and Coulomb interactions and enable a valid comparison with HIJING. The results indicate that the width of the balance function for peripheral events is consistent with that expected from HIJING, while the width for central events is significantly smaller as was observed with charged particle pairs.

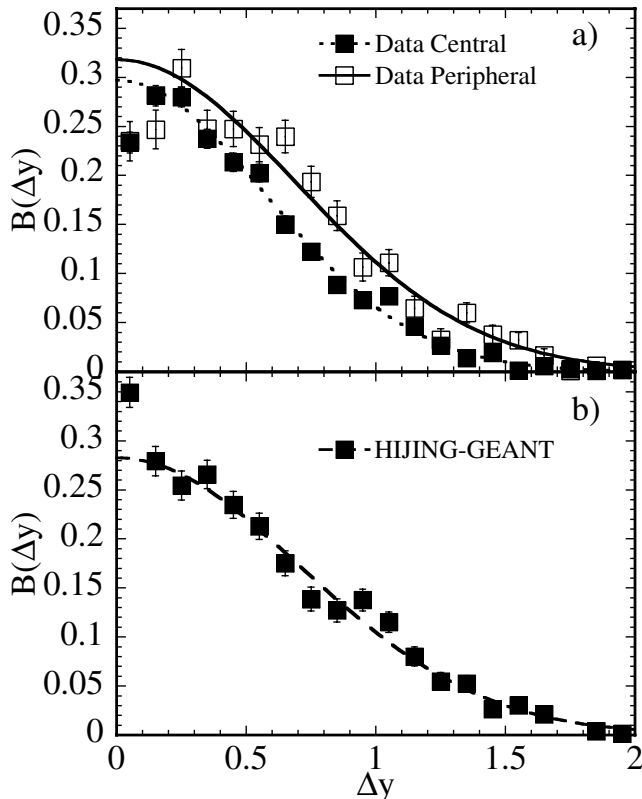


FIG. 3. The balance function versus Δy for identified pion pairs from (a) central and peripheral Au + Au collisions at $\sqrt{s_{NN}} = 130$ GeV, and (b) HIJING events simulated in GEANT [16]. To guide the eye, Gaussian fits excluding the lowest two bins in Δy are shown. The error bars shown are statistical. The balance function for HIJING events is independent of centrality.

To gain some insight into the observed widths in central collisions, we compared with the thermal model (final temperature of 165 MeV) presented in [8] filtered through the acceptance of STAR. We find that the predicted widths are larger than those we observe in central collisions. Thermal model calculations have also been done at low final temperature (105 MeV) and high transverse velocity ($0.77c$), while maintaining the same average transverse momentum. These calculations predict a balance function width consistent with our observations in central collisions. Thus, the observed narrowing of the balance function in central collisions can be parametrized in a thermal model that incorporates strong transverse flow and is constrained to emit the balancing particles close together in space-time [20]. This constraint could arise from delayed hadronization compared with the characteristic 1 fm/ c hadronization time or from some other phenomena such as anomalously short diffusion of particle pairs [20]. Other phenomena besides flow may also affect the width of the balance function as a function of centrality such as resonance decay or the effects of the nuclear medium on jetlike correlations.

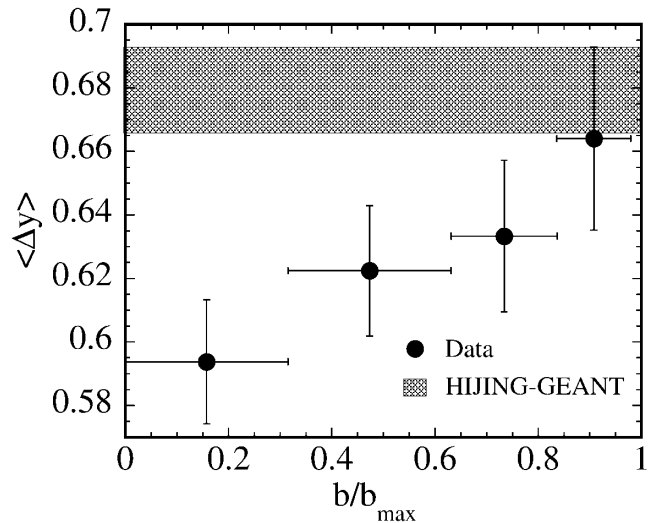


FIG. 4. The width of the balance function for identified charged pions, $\langle \Delta y \rangle$, as a function of normalized impact parameter (b/b_{max}). Error bars shown are statistical. The width of the balance function from HIJING events is shown as a band whose height reflects the statistical uncertainty.

In summary, measurement of the balance function for Au + Au collisions at $\sqrt{s_{NN}} = 130$ GeV has been stimulated by the prediction [8] that the width of the balance function should be significantly reduced by late hadronization. We indeed observe a narrowing of the balance function for more central collisions for all charged particle pairs and for charged pion pairs. Only for peripheral collisions is the width consistent with HIJING predictions treating the Au + Au collision as a superposition of independent nucleon-nucleon scatterings. Interpretation of the observed narrowing requires more detailed study of its sensitivity to such other effects as flow, resonance production, and diffusion, in addition to late hadronization.

We wish to thank the RHIC Operations Group and the RHIC Computing Facility at Brookhaven National Laboratory, and the National Energy Research Scientific Computing Center at Lawrence Berkeley National Laboratory for their support. This work was supported by the Division of Nuclear Physics and the Division of High Energy Physics of the Office of Science of the U.S. Department of Energy, the U.S. National Science Foundation, the Bundesministerium fuer Bildung und Forschung of Germany, the Institut National de la Physique Nucleaire et de la Physique des Particules of France, the United Kingdom Engineering and Physical Sciences Research Council, Fundacao de Amparo a Pesquisa do Estado de Sao Paulo, Brazil, the Russian Ministry of Science and Technology, the Ministry of Education of China, the National Natural Science Foundation of China, and the Swiss National Science Foundation.

- [1] J.W. Harris and B. Müller, *Annu. Rev. Nucl. Part. Sci.* **46**, 71 (1996).
- [2] S. A. Bass, M. Gyulassy, H. Stöcker, and W. Greiner, *J. Phys. G* **25**, R1 (1999).
- [3] S. Jeon and V. Koch, *Phys. Rev. Lett.* **85**, 2076 (2000).
- [4] M. Asakawa, U. Heinz, and B. Müller, *Phys. Rev. Lett.* **85**, 2072 (2000).
- [5] Zi-wei Lin and C. M. Ko, *Phys. Rev. C* **64**, 041901 (2001).
- [6] H. Heiselberg and A. D. Jackson, *Phys. Rev. C* **63**, 064904 (2001).
- [7] E.V. Shuryak and M. A. Stephanov, *Phys. Rev. C* **63**, 064903 (2001).
- [8] S. A. Bass, P. Danielewicz, and S. Pratt, *Phys. Rev. Lett.* **85**, 2689 (2000).
- [9] ACCDHW Collaboration, D. Drijard *et al.*, *Nucl. Phys.* **B166**, 233 (1980).
- [10] TPC/Two Gamma Collaboration, H. Aihara *et al.*, *Phys. Rev. Lett.* **53**, 2199 (1984).
- [11] STAR Collaboration, M. E. Beddo *et al.*, LBL PUB-5347 (1992).
- [12] W. Betts *et al.*, *IEEE Trans. Nucl. Sci.* **44**, 592 (1997); H. Weiman *et al.*, *IEEE Trans. Nucl. Sci.* **44**, 671 (1997).
- [13] C. Adler, A. Denisov, E. Garcia, M. Murray, H. Ströbele, and S. White, *Nucl. Instrum. Methods Phys. Res., Sect. A* **461**, 337 (2001).
- [14] M. Calderon, Ph.D. dissertation, Yale University, 2001.
- [15] X. N. Wang and M. Gyulassy, *Phys. Rev. D* **44**, 3501 (1991).
- [16] CERN Program Library, Long Writeups Q123, Application Software Group, 1993.
- [17] M. B. Tonjes, Ph.D. dissertation, Michigan State University, 2002.
- [18] S. Jeon and S. Pratt, *Phys. Rev. C* **65**, 044902 (2002).
- [19] J. Gosset *et al.*, *Phys. Rev. C* **16**, 629 (1977).
- [20] S. Pratt and S. Jeon, *Proceedings of the 18th Winter Workshop on Nuclear Dynamics*, edited by R. Bellwied, J. Harris, and W. Bauer (EP Systema, Debrecan, Hungary, 2002), p. 91.